Evaluation of icephobic coatings—Screening of different coatings and influence of roughness

CrossMark

Markus Susoff, Konstantin Siegmann, Cornelia Pfaffenroth, Martina Hirayama*

Zurich University of Applied Sciences, School of Engineering, Institute of Materials and Process Engineering, Technikumstrasse 9, CH-8400 Winterthur, Switzerland

A R T I C L E   I N F O

A B S T R A C T

Icing of wind turbines affects energy production, causes mechanical failures and increases safety hazards in general; hence there is an enormous demand for powerful anti-icing methods. To investigate the icephobic properties of different coatings, ice adhesion measurements were performed with a 0° cone test to determine ice adhesion strengths between coating and ice. Various coatings with different icephobic properties were investigated, e.g., hydrophilic and hydrophobic coatings, sol–gel based coatings containing fluorinated compounds and viscoelastic rubbers, as well as commercially available icephobic products. The coatings currently used on wind turbines showed an adhesion to ice that is comparable to that of bare aluminium; meaning a quite high adhesion to ice. Very low adhesion values were obtained in the case of coatings consisting of viscoelastic elastomers. Additionally, the influence of surface roughness on ice adhesion has been examined. Aluminium pins were chemically and mechanically roughened and their ice adhesion was determined. These pins were further coated with a fluorine-containing coating in order to study the influence of minimized surface energies. Shear stress of those coated pins was considerably reduced, however, rough surfaces showed higher ice adhesion than smooth ones.

1. Introduction

Ice accretion and ice adhesion on different surfaces can result in severe problems on power lines, telecommunications, transportation in general, aircraft or power production by wind turbines. Icing of wind turbines not only affects their energy production performance, but also causes mechanical and electrical failures, influences monitoring and controlling, as well as generating safety hazards. About 20% of all wind turbines are located at sites where icing events are likely to occur during winter. The resulting power losses can be up to 50% of the annual production [1]. The reason for building wind turbines in these regions is based on the fact that the available wind power is 10% higher than in other regions. In Switzerland, the most suitable sites for wind turbines are located more than 800 m above sea level, and these locations often face extremely harsh conditions [2]. Hence, there is an enormous demand for powerful methods to keep wind turbines ice-free. These methods can be divided into anti- and de-icing ones [1]. Anti-icing systems try to avoid ice accretion whereas de-icing methods are applied when ice already has built up. Our research focuses on a passive method, namely permanent icephobic coatings, which decrease the adhesion of ice to a surface in such a way that accreted ice may fall off from the rotor blades due to accreted mass, combined with centrifugal and vibrational forces alone. In contrast to active anti- and de-icing methods, passive ones do not need any external power such as heating systems or the like; they take advantage of their physical surface properties. Besides their anti-ice properties, these coatings should be inexpensive, durable and easy to apply.

Although lots of studies were made in the field of icephobic coatings, the determination of ice adhesion is still a challenge. The comparison between different measuring methods is restricted in terms of strain rates that are used as well as different forces that occur between ice and the coatings. Very promising results are given by the 0° cone test, which is easy to prepare and to operate [3–5]. We used a modification of this test method because it allows the measurement of the adhesive strength of different coatings and bare materials with high reproducibility. This universal ice adhesion test is applicable for the determination of icephobic properties of various coatings. A suitable measure for this ice adhesion is the so-called adhesion reduction factor (ARF) that allows for comparison of results obtained by different measuring methods.

* Corresponding author. Tel.: +41 58 934 7326; fax: +41 58 935 7326.
 E-mail address: martina.hirayama@zhaw.ch (M. Hirayama).

An approach to find a correlation between the water wettability of certain surfaces and their ice adhesion strengths provided no clear correlation, however, Meuler et al. found a promising dependency of ice adhesion on the receding contact angle [6]. It was studied if increasing the contact angle into the superhydrophobic regime ($\Theta > 150°$) could lead to lower ice adhesion due to the water-repellent properties of superhydrophobic surfaces. Many studies can be found reporting a reduction of ice adhesion as well as delayed ice accretion by using superhydrophobic surfaces [7–12]. Contrary to these studies, recent investigations provided disputable results concerning the use of superhydrophobic coatings as icephobic surfaces [13–16]. Structuring surfaces means changing their topography, hence, superhydrophobic surfaces always show a certain roughness. While roughness has a major influence on ice adhesion [17,18], this can be the reason for the questionable use of superhydrophobic surfaces in the field of icephobic coatings. In sum, there is still a lack of concensus in the literature whether a correlation between wettability and ice adhesion exists at all, and it is still doubtful if superhydrophic surfaces show a general icephobic behaviour under different icing conditions.

In this study, we performed a screening of a variety of different coatings to supplement the discussion about the relationship between wettability and ice adhesion. Therefore, we investigated synthesized coatings as well as six standard commercially available coatings currently used on the rotor blades of operating wind turbines. In addition, the influence of different degrees of roughness of the coatings on ice adhesion was investigated. Additionally, we generated rough but low-energy surfaces to systematically study the interplay between low-energy surfaces, roughness and ice adhesion. The objective was to understand the influence of wettability and roughness on ice adhesion to develop a permanent icephobic coating that produces lower ice adhesion than what has been already reported in literature, knowing that icing cannot be completely avoided.

2. Materials and methods

2.1. Preparation of coatings

All sol–gel coatings were synthesized by using silica precursors consisting of tetraethylorthosilicate (TEOS, Aldrich) and (3-glycidylpropyl)trimethoxy silane (GPTMS, Aldrich) in different ratios. Diluted hydrochloric acid was used as a catalyst.

Different additives bearing alkoxy silane groups were added to this silica precursor system to impart different properties to the coating. "Fluorolink®S10" (ABCR, Germany) is a α,ω-triethoxysilane terminated polyfluorinated polyether (PFPE) with a molecular weight of ~2000 g/mol. Fluorolink®S10 can be represented as follows:

$(EtO)_3Si—CH_2CH_2CH_2—NH—CO—CF_2O(CF_2CF_2O)_m—(CF_2O)_n$

$—CF_2—CO—NHCH_2CH_2CH_2—Si(OEt)_3$
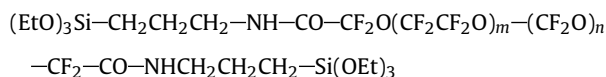
The other fluorinated compound used in this study was "Fluorotelomer-V" (Clariant, Switzerland). It bears just one triethoxysilane group and possesses a molecular weight of ~2900 g/mol:

$(EtO)_3Si—CH_2CH_2CH_2—NH—CO—CF_2(O—CF_2—CF(CF_3))_m$

$—O—CF_2—CF_2—CF_3$
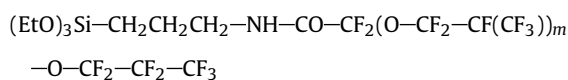
For the synthesis of coatings containing Fluorolink®S10 ("sol–gel fluorinated 1a–c") 9.3 g TEOS and 3.9 g GPTMS were given to a mixture of 12 ml tetrahydrofuran (Aldrich) and 12 ml ethanol (Haeseler, Switzerland), then 0.4 g, 0.8 g or 1.6 g Fluorolink®S10 was

added in either 1 wt%, 2 wt% or 3 wt%. Hydrolysis was started by adding a mixture of 1.2 g HCl (conc.) and 4.4 g H_2O under ice-cooling of the reaction vessel. The solution was stirred for one day at ambient temperature. After dip-coating the substrates (aluminium pins and platelets), the coatings were cured for 1 h at 120 °C.

"Sol–gel fluorinated + Aerosil 1d and e" coatings showing contact angles of 134° and 169° were prepared by incorporating different amounts of silica particles (Aerosil R805) to the coating solutions.

Coatings containing Fluorotelomer-V ("sol–gel fluorinated 1g–i") were prepared in a similar method as for the ones with "Fluorolink®S10", except Fluorotelomer-V was used instead of "Fluorolink®S10". "Sol–gel fluorinated 1j–n" are coatings that contain "Fluorolink®S10" as well as "Fluorotelomer-V" in different ratios. Additionally, the coating "sol–gel fluorinated 1f" was prepared by adding 1.1 g "Fluorotelomer-V" to 10.5 g GPTMS in 17.5 g isopropanol. For hydrolysis 10.5 g of 0.03 mol/l HCl were added and the reaction mixture was stirred for 48 h. The coating was applied by dip-coating and the curing was done at 120 °C for 1 h.

Siliclad® Glide 10 (ABCR, Germany) was applied as 2 and 5 wt% solution in isobutyl acetate (Haeseler, Switzerland). Dynasylan® 4144 (Evonik, Germany) (used to introduce polyethylene glycol (PEG) to the silica matrix) was applied as recommended in the technical data sheet. N-Trimethoxysilylpropyl-N,N,N-trimethylammoniumchlorid (Aldrich) (used as an ionic component) was applied according to a report in literature [19].

For coatings prepared from viscoelastic elastomers, a two component silicone system was used that cures by an addition-crosslinking reaction. This silicone rubber shows a Shore A hardness of 25 and an elastic modulus of $G' = 440,000$ Pa at 100 °C at a measuring frequency of 1 Hz. For the application on aluminium an adhesion promoter was used. According to Hirayama et al., poly(hydrogenmethylsiloxane) was used as a primer [20]. The coatings were applied by dip-coating using solutions of this silicone in toluene and cured at 100 °C for 1 h.

Nusil R-1009® was purchased directly from Nusil-Silicones. Nusil R-1009® is a one-component condensation curing silicone system that does not need any adhesion promoter. The coating was applied by dip-coating from a 50 wt% solution in toluene. The coating was cured for two days at ambient temperature in the presence of air humidity.

All chemicals were high purity reagents and were used as received without further purification.

All coatings were applied by dip-coating process on cleaned and plasma activated aluminium pins and platelets. For this, a dip-coater (KSV dip coater, LOT Oriel) was used to coat the substrates automatically. For each coating, the platelets were held for 30 s in the respective solution, and were pulled out of the solution with a constant velocity of 300 mm/min. Then, the coatings were cured as previously described.

The standard wind turbine coatings were applied directly onto aluminium pins by the coating manufacturer.

Teflon coated aluminium pins were prepared by Eposint AG, Switzerland.

2.2. Contact angle measurements

Static contact angles of deionized water (Millipore) were measured with a DSA-10 goniometer (Krüss, Germany) at room temperature by applying water droplets of 6 μl onto the respective surfaces. Dynamic sessile water drops were observed using the drop shape analysis (DSA) system (DSA-100, Krüss, Germany) combined with the analytical software (DSA4, Krüss, Germany) and equipped with a high speed camera. Advancing (θ_{adv}) and receding (θ_{rec}) angles were measured as water was supplied via a syringe into or out of sessile droplets. Starting drop volume for

determination of θ_{adv} was between 2 and 5 µl and between 20 and 100 µl for determination of θ_{rec}, depending on surface coating. The drop shapes have been recorded every 2 s during an evaluation period depending on final droplet size. A minimum of five measurements on different spots was recorded for each substrate.

2.3. Preparation of different degrees of roughness on aluminium plates

The aluminium pin material was of the type "Anticorodal" (Anticorodal-112, EN AW-6082 AlSi1MgMn, Allega GmbH, Switzerland), whose surface roughness could be altered in many ways. Different degrees of roughness can be obtained chemically, by etching with acid or alkali, or mechanically, by roughening by sand blasting or abrasive paper. In this study, diluted hydrochloric acid was used for chemical roughening. Other pins were roughened by sand blasting. Further, pins were treated with abrasive paper in such a way that roughness showed a preferred orientation perpendicular to the pin axis.

Chemical etching was performed by using diluted hydrochloric acid, formed by diluting concentrated hydrochloric acid in a 1:3 ratio with demineralized water. At room temperature, the degreased and cleaned pins were put into the stirred mordant. The time after which the pins were removed from the mordant depended on the course of the reaction. Aluminium dissolves exothermally in hydrochloric acid, therefore the solution becomes warm and this in turn accelerates the reaction. However, before the reaction starts there is a time delay because the oxide layer has to first be dissolved. The etching time was chosen to be either 5 min, or between 10 and 15 min. In conclusion, it should be noted that there is an induction period until the aluminium gets dissolved. However, relatively high roughness in the range of a few micrometres can thus be obtained.

2.4. Determination of roughness

Roughness was analyzed in terms of surface roughness S_a by a confocal microscope (Leica DCM 3D, Germany). The surface area investigated was in most cases 255×191 µm^2. For determination of surface roughness it has to be considered that the samples show a curvilinear surface. Therefore the analysis of these samples was done by Leica software (Leicascan DCM 3D Version: 3.2.0.9) which allows for assuming a plane surface via a mathematical transformation. Roughness was determined at different positions along the pin, and at least five measurements were performed for each sample.

2.5. Ice adhesion measurements: test geometry and procedure

For the determination of the adhesive strength on ice, we utilized a standard testing method in accordance to Haehnel and Mulherin [3]. They adapted the 0° cone test for measuring the adhesive strength of ice in shear. The test setup consists of an inner cylindrical pin and an outer cylindrical mould. The pin is centred in the mould that possesses a notch at the bottom that fits to the pin's diameter. The annular gap between pin and mould is filled with deionized water and the whole test block is put into a deep freezer overnight to allow the water to freeze at temperatures $T < -25\,^\circ$C. For measuring the adhesive strength the pin is pulled out of the mould by a tensile testing machine at $-14\,^\circ$C, putting the ice into shear. This procedure differs from the one of Haehnel and Mulherin. In their approach, the pin is loaded axially to put it in shear. Whichever method is used, shear forces between ice and pin are produced showing only a difference in the algebraic sign.

The shear stress τ can be described by the following equation:

$$\tau = \frac{P}{A} = \frac{P}{\pi D c} \tag{1}$$

where P is the applied load, A is the surface area of direct contact to the ice, D is the diameter of the pin and c describes the height of the mould. The strain rate $\dot{\varepsilon}$ can be calculated in the following way [3]:

$$\dot{\varepsilon} = \frac{1}{2} \frac{u_z}{a} \tag{2}$$

where u_z is the vertical velocity of the pin and a is the annular gap between the pin and the mould.

The details of the test geometry and its stress analysis are given in depth by Haehnel and Mulherin [3,4].

Since temperature significantly affects ice adhesion, the mould is equipped with a temperature sensor that measures the temperature at the ice–mould interface. All measurements were performed at $-14\,^\circ$C. After adjusting the test block to the tensile testing machine, it was allowed to warm-up until the desired temperature was reached before starting the measurement process. The tensile velocity was in most cases $u_z = 1$ mm/min resulting in a strain rate of $\dot{\varepsilon} = 2.78 \times 10^{-3}$ s^{-1}. Fig. 1 shows the setup of the mould and the frozen-in pin at the testing machine. The test block is fixed at the bottom, and on the top the pin is clamped to be pulled out of the ice with a constant velocity.

For the determination of adhesion strengths, the force of load vs. displacement of the pin is measured at a constant tensile velocity. The force increases in a nearly linear and continuous way until the adhesion between ice and the surface fails and the force decreases to zero after a sharp kink. The maximum load is used to calculate the shear stress by dividing the maximum load by the surface area (aluminium pin with diameter $D = 2$ cm; surface area that is in contact with the ice $A = 0.0037$ m^2).

For the comparison of results obtained by different test methods, the shear stress alone is not an appropriate term because the shear stress is strain rate dependent. It is more reasonable to normalize the results by a reference shear stress obtained with a certain material. In many cases, aluminium was used as this reference [3,11,17,21,22]. By normalizing one gets the so-called adhesion-reduction-factor (ARF), given by the following equation:

$$ARF = \frac{\tau_{Alu}}{\tau_{coating}} \tag{3}$$

where τ_{Alu} is the shear stress of bare aluminium and $\tau_{coating}$ the shear stress of the sample under investigation. Hence, the ARF of the reference (bare aluminium) equals one. The ARF is a measure of the ability of a certain coating to reduce the adhesion to ice compared to bare aluminium. Thus, high ARF values mean low adhesive strengths of the coated surface.

3. Results and discussion

3.1. Evaluation of the ice adhesion test

The dependence of shear stress on strain rate is due to relaxation processes of either the material (or coating) or of the ice itself. It was shown that shear stresses for stainless steel increased with strain rate until a plateau was reached [3]. This behaviour was observed for strain rates in the range of 10^{-5}–10^{-3} s^{-1} by using a 0° cone test. Even lower strain rates down to 10^{-6} s^{-1} occur by using the centrifuge adhesion test [23].

For a better understanding of our test set up, we conducted an analysis of the stress–strain rate relationship of two different materials at somewhat higher strain rates. As a purely elastic material we chose aluminium (uncoated aluminium pin) and a silicone rubber was chosen as a viscoelastic coating. Silicone as an icephobic
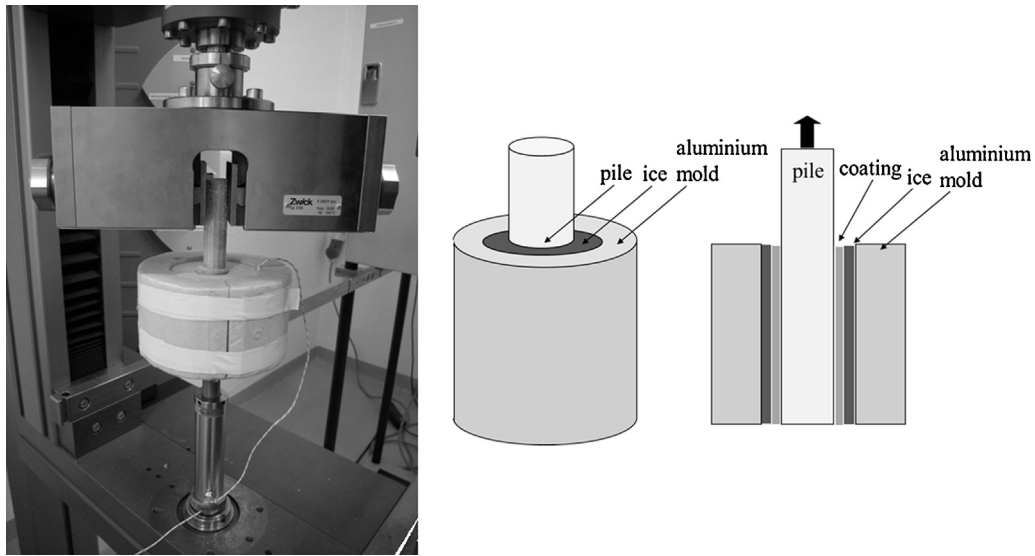
Fig. 1. Ice adhesion test setup. Left: adjustment of mould and corresponding frozen-in pin at tensile testing machine; right: sketch of the ice adhesion test setup.

material is promoted by Nusil® showing very low shear stresses [24]. In our test setup we were able to increase the strain rate. A decrease of the strain rate would have meant that the samples are exposed to longer measuring times resulting in an increase of the measuring temperature. Hence, the tensile velocity was increased from 1 mm/min to 20 mm/min, producing strain rates of 2.78×10^{-3}–5.56×10^{-2} s^{-1}, respectively.

In Fig. 2 it can be seen that a significant dependence exists between the shear stress of the silicone coating on the strain rates. By increasing the strain rate the changes in shear stress become smaller, hence a plateau value can be expected at even higher strain rates. Only small changes of the shear stress with strain rate are observed in the case of bare aluminium. It can be concluded that the plateau region is already reached for these strain rates.

The behaviour depicted in Fig. 2 can be explained by the fact that aluminium as a metal shows only pure elastic behaviour (Young's modulus: ≈70 GPa). Thus, any dependence of the shear stress on strain rate should be due to the viscoelastic properties of ice showing a Young's modulus of about 9 GPa. However, this behaviour can only be observed at very low strain rates because those relaxation processes emerge only after long times. Contrarily, silicone rubber possessing a Young's modulus below 0.1 GPa shows those dependencies already at shorter times, meaning higher strain rates. Thus,

the behaviour is primarily dominated by the silicone's viscoelastic properties in comparison to those of ice. However, increasing the strain rate should also in this case end in a strain rate-independent region.

Reflecting on these results with regard to the stress–strain relationship and influence of other parameters, the strain rate should be a fixed value if dealing with ice adhesion measurements by tensile tests. Aside from the geometry of the setup and the temperature, the strain rate is a parameter that possesses an enormous influence on ice adhesion. Whether a strain rate-dependency exists or not depends on the materials or coatings used. Additionally, the influence of the system "ice" may not be disregarded although it only appears at low strain rates.

In order to verify the suitability of our method for the determination of ice adhesion, a test series of 25 samples of bare aluminium was carried out to prove reproducibility. For each measurement an unused aluminium pin was frozen into the mould. After freezing overnight, the pin was pulled out with a velocity of 1 mm/min. Fig. 3 shows the shear stress of the specimens.

The mean shear stress is $\tau = 1573 \pm 191$ kPa visualized by the broken line in Fig. 3. This value fits well to the literature data, although a higher strain rate was used [3]. This fact indicates that the rate-independent region is reached. The standard deviation is
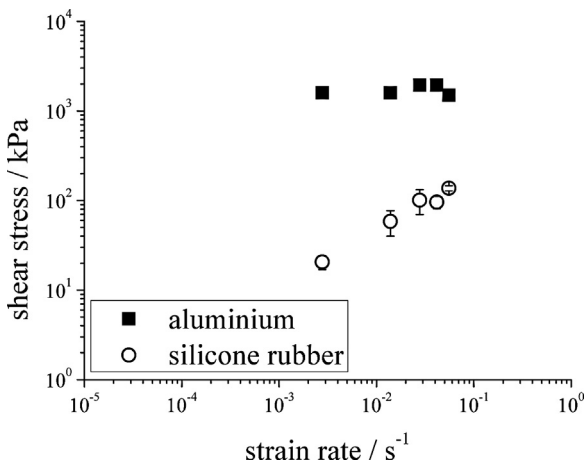

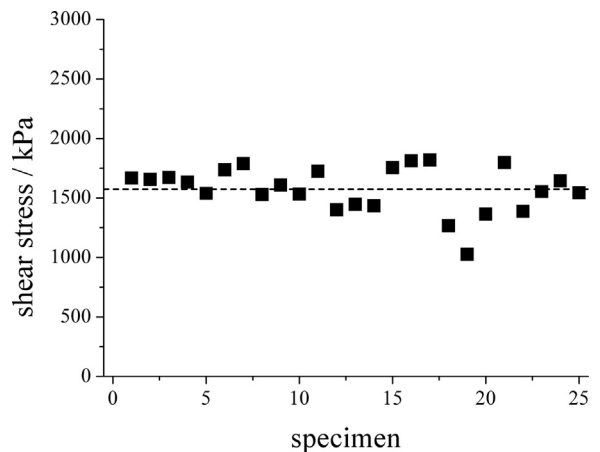**Fig. 2.** Dependence of shear stress of bare aluminium and silicone coated aluminium on strain rate.

Fig. 3. Course of shear stress for a test series consisting of 25 specimens (bare aluminium) at a velocity of 1 mm/min.
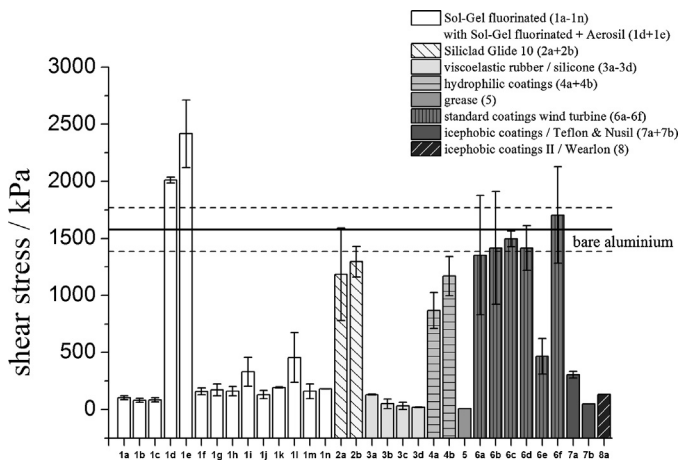
Fig. 4. Screening of different coatings. Shear stress of investigated coatings that are classified into certain groups; horizontal line denotes mean shear stress of bare aluminium (reference material), dotted line = standard deviation; shear stress value of Wearlon was calculated.

12%, signifying a quite good reproducibility. The deviations and scattering of the data points can be attributed to the manufacturing of the aluminium pins and small deviations in their surface roughness.

In general, the measurements show that the method applied here for the determination of ice adhesive strength provides reliable data and good reproducibility.

3.2. Ice adhesion of coatings

Since ice accumulation has an enormous impact on transportation (roads, boats, airplanes) and energy production (e.g., energy losses of wind turbines due to icing), a variety of so-called "icephobic" coatings and paints are commercially available. Teflon (polytetrafluorethylene) is known as the "best" icephobic material, so it was reasonable to determine its adhesive strength with our adhesion test [25]. In literature, its ARF value is given as 5–7. In our study, we determined an ARF value of ≈5 according to a shear stress of about 305 kPa (Fig. 4, coating 7a). Additionally, the shear stresses of the commercially available icephobic coating Wearlon® (coating 8a), and a silicone based coating of Nusil® (coating 7b) are added to Fig. 4, where the value for Wearlon® was calculated from literature data [26], denoted as "icephobic II". Wearlon® is a combination of epoxy and silicone compounds. In 2004 it was considered to be the best non-sacrificial icephobic coating providing an ARF value of 12 [26]. Very promising results are given by Nusil Silicone Technology that distributes silicone based coatings for the prevention of icing on different surfaces (www.nusil.com). Some of these coatings comprise fluorosilicones that should give coatings with very low surface energies. In our study the ARF of Nusil R-1009 was determined. If the shear stresses of the commercial coatings are compared to all other analyzed coatings, it can be concluded that Wearlon® possesses quite good but no exceptional icephobic properties. In contrast, the Nusil product in general seems to possess very good icephobic properties.

For protecting the rotor blades on wind turbines, so called erosion resistant paints are used. They are often based on polyurethanes, thus they possess a slightly hydrophilic character and act as long lasting erosion protection finishes. These coatings prevent the erosion of the blades due to particles and other impurities that are present in air. Some manufacturers also promote their products as icephobic ones. Six "state of the art" coatings from the wind turbine industries were analyzed with regard to their icephobic properties. They are labelled as "standard coatings wind turbine

6a–f". It can be seen in Fig. 4 that their adhesion to ice is as high as it is for bare aluminium. Only one coating shows a significant lower shear stress resulting in an ARF of three. From their static water contact angles, these coatings also show fairly hydrophilic characteristics leading to better adhesion of water.

In addition to the determination of the ice adhesion of commercially available products, it was the aim of this study to develop new coatings or to modify systems that are already used in the field of adhesion reducing materials.

New systems were developed comprising coatings that are based on sol–gel chemistry containing the fluorinated components Fluorolink®S10and Fluorotelomer-V. In all cases the fluorinated compounds consist of perfluorinated polyether bearing one (Fluorotelomer-V) or two (Fluorolink®S10) trialkoxy silane end-groups to be directly incorporated in the sol–gel network. "Sol–gel fluorinated 1a–c" comprises coatings with Fluorolink®S10 [27]. In contrast to the latter coatings, "sol–gel fluorinated 1f–i" are made of silica precursors TEOS and GPTMS and Fluorotelomer-V. The series of "sol–gel fluorinated 1j–n" is a combination of both fluorinated polyethers. It can be seen that the coatings consisting only of Fluorolink®S10 (sol–gel fluorinated 1a–c) show the lowest ice adhesion of this group. The ARF-value is about 20, this means that the adhesion of ice to these coatings is 20 times lower than to bare aluminium. The static contact angle of water on this coating of nearly 120° is in the hydrophobic regime. The use of Fluorotelomer-V or the combination of Fluorolink®S10and Fluorotelomer-V within the silica network does not reduce the shear stress any further. By incorporating fumed silica particles (Aerosil R805) to the coatings containing Fluorolink®S10, even more hydrophobic surfaces are obtained due to the structured and low energy surface. However, these coatings "sol–gel fluorinated aerosil 1d + e" with static contact angles of 134° and 169° respectively show an enormous increase in adhesive strength to ice, especially the superhydrophobic "sol–gel fluorinated Aerosil 1e" (static water contact angle: 169°). The shear stress exceeds the ice adhesion of aluminium by more than 50%. Although this aspect was only analyzed for one single type of coating, it indicates the use of superhydrophobic coatings as potentially icephobic surfaces is disputable.

The second group of coatings is based on a siloxane modified polysilazane (Siliclad® Glide 10, coatings 2a + b) that forms covalent bonds to substrates like metal or glass. This product gives a coating with a static water contact angle in the hydrophobic regime (104°). The ice adhesion was measured for two concentrations (2 and 5 wt% in butyl acetate; denoted "siliclad glide 10 2a" and "siliclad glide 10 2b" respectively). The results show that the adhesive strengths to ice are very high, above 1000 kPa and giving ARF values close to one.

"Viscoelastic rubber 3a–d" are coatings prepared from polydimethylsiloxanes. The combination of their low surface energy and their outstanding elasticity qualifies these elastomers for application as icephobic materials. Due to their anti-adhesive properties, an adhesion promoter has to be used to create a permanent bond between coating and substrate [20]. The shear stresses of the polydimethylsiloxane coatings are very low and give accordingly high ARF values. However, significant drawbacks of these coatings are certainly their poor mechanical properties. Due to their high elasticity, polydimethylsiloxane elastomers are soft and not resistant against erosion. This is in contrast to the coatings based on silica networks and Fluorolink®S-10 that show good mechanical properties alongside their acceptable icephobic properties [28–30].

Besides these hydrophobic coatings, hydrophilic sol–gel coatings were investigated. Dynasylan 4144® was used to introduce PEG chains into the silica matrix ("Sol–Gel PEG") (coating 4a). As an example for a sol–gel coating containing ionic functionalities, a quaternary ammonium salt with alkoxy silane groups was used in combination with TEOS and GPTMS (coating 4b). Both

coatings show shear stresses around 1000 kPa indicating no ice-phobic behaviour. This can be traced to their hydrophilic properties that enhance the adhesion of water molecules to the surface.

When aluminium pins are used as substrate material, the coatings described are either bonded directly to the aluminium or a primer has to be used. Hence, these coatings are permanent. In contrast, lithium grease as an non-permanent coating was analyzed. This grease acts as a lubricant and the ARF value is far in excess of 100. However, it cannot be said that ice is released from the coating in an adhesive way, as most of the grease remains on the ice surface. Such non-permanent coatings or films can also be analyzed by our custom-made adhesion test.

To summarize, by analysing the adhesive strengths of different coatings to ice, the measured shear stress varies significantly depending on the nature of the surface. Very low shear stresses were determined in the case of coatings based on sol–gel chemistry with a perfluorinated polyether like Fluorolink®-S10. Further coatings of the same kind that differ only in the composition of the fluorinated additives also show low ice adhesion, but they cannot markedly decrease the ice adhesion. A drastic increase of the shear stress is obtained as soon as silica particles like Aerosil® are added to the coatings, resulting in superhydrophobic surfaces. Very high shear stresses are measured in the case of hydrophilic coatings, and they do not show any potential in reducing ice adhesion. Also, only low ARF-values are obtained for the fairly hydrophobic coatings made from Siliclad® Glide 10. The investigated impermanent coatings show a different behaviour, films made of lithium grease release ice easily and shear stresses below 10 kPa were measured.

Six different state of the art wind turbine coatings from two companies were also analyzed in our study. The lowest measured shear stress was about 500 kPa resulting in an ARF value of 3. The other coatings showed significant higher adhesive strengths to ice comparable to bare aluminium, indicating no icephobic character at all for these kinds of coatings.

Viscoelastic coatings based on polydimethylsiloxane showed the best icephobic behaviour. These silicone coatings provide ARF-values up to 100 indicating an enormous potential for further improvements.

After the determination of the shear stresses and respective ARF values, it seems obvious to look for a correlation between the adhesive strength and another parameter, e.g., the wettability of the surface, to be able to explain and possibly predict the icephobic character of the respective coating. Different kinds of water contact angle measurements allow statements about the surface chemistry and give therefore the opportunity to characterize the interface of the coating that is in contact with water or ice. Besides the static (or equilibrium) contact angle, also the advancing and receding contact angles are of certain interest as the so called contact angle hysteresis can be determined from them giving additional information about the roughness of surfaces.

In Fig. 5 the ARF values are plotted versus the static contact angle of water. This diagram shows two types of data. The filled squares are data points taken from the Anti-icing Materials International Institute (AMIL, Chicoutimi, University of Quebec, Canada), the open circles belong to the coatings measured in this study [31]. At the AMIL, the adhesive strength to ice is analyzed by a centrifuge ice adhesion reduction test, hence the strain rates are smaller than in our study. However, normalizing the values for shear stress with aluminium provides ARF-values that can be compared to other ARF-values determined by different test methods.

Regarding the static contact angle of water, one can distinguish roughly three different regions: coatings that cover the hydrophilic range (Θ = 0–90°), coatings that are situated in the hydrophobic regime (Θ = 90–140°) and superhydrophobic coatings (Θ > 140). On the ordinate, the ARFs are plotted on a logarithmic scale. Following
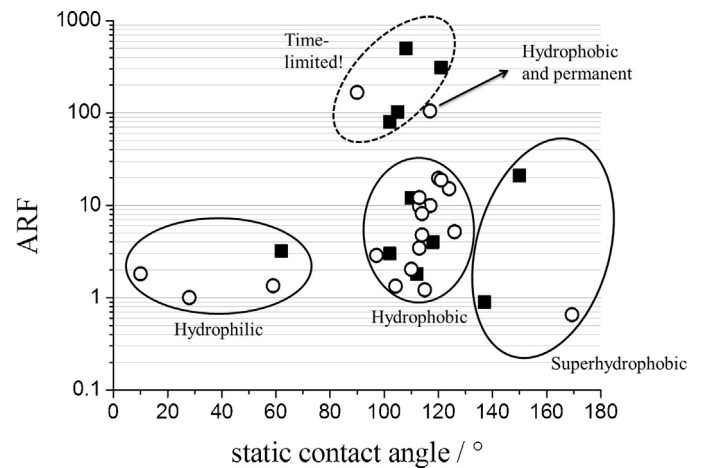

Fig. 5. Adhesion-reduction-factors (ARF) dependence on water contact angle. ○: data determined in this study, ■: data taken from AMIL [31].

a rough estimation of AMIL, an ARF value of 100 is needed to reach the self-deicing minimum. An ARF value of one corresponds in our case to bare aluminium as the reference material.

The hydrophilic coatings with contact angles between 10° and 60° show only little reduction of ice adhesion. Probably, the water molecules experience an increased attraction because of the polar character of the hydrophilic coating leading to stronger adhesive bonding.

The hydrophobic regime covering contact angles between 90° and 120° shows the largest variation of measured ARF values. Most of these hydrophobic coatings possess ARF values between 1 and 20, comparable to the hydrophilic group. Besides this regime, other hydrophobic coatings show ARF values close to and above 100. These coatings have only weak adhesion to ice and can be characterized as very icephobic coatings. Unfortunately, most of them are non-permanent coatings. This means that they have a limited lifetime after which the coating has to be renewed, e.g., powder coats or greases that are sacrificial coatings. However, one permanent coating included in our study showed a very high ARF value. Although the data of AMIL and ZHAW coincide in most cases, this hydrophobic and permanent coating possesses exceptionally low adhesion to ice. This coating is made of polydimethylsiloxane and it is possible that even higher ARF-values can be found by optimizing the coating composition and application process.

Contact angles higher than 120° can only be realized by a surface with low surface energy in combination with a certain structured topography [6]. The region covering contact angles higher than 140° is the superhydrophobic regime. In literature there is still much discussion concerning the correlation between superhydrophobicity and icephobic character. Regarding the ARF values of ZHAW and AMIL in this regime, one ARF value is above ARF = 1, and two others show ARF < 1 meaning that they have a stronger adhesion to ice than bare aluminium. This can be due to the structured surface that can act as an anchor for ice, so that the adhesive strength increases enormously.

Meuler et al. stated that the ice adhesion strength correlates more strongly with either the roll-off angle for water drops or the practical work of adhesion of water than it does with the static contact angle [6]. They investigated the ice adhesion strengths on 21 different materials showing smooth surfaces and focused on the relationship between ice adhesion and water wettability. Meuler et al. found a strong correlation between the average strength of ice adhesion and the practical work of adhesion scaling parameter $(1 + \cos\theta_{rec})$ with θ_{rec} representing the receding contact angle. Increasing the receding angle should result in decreased ice adhesion strength. From their conclusion, the icephobicity of
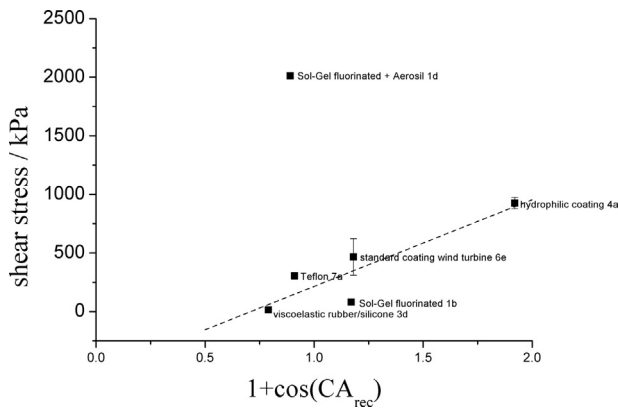
Fig. 6. Ice adhesion strength in dependence of $(1 + \cos(CA_{rec}))$ for six coatings with denotations taken from Fig. 5. CA_{rec}: receding contact angle.

Table 1
Roughness (S_a) due to different processing methods.

Method of processing	Roughness (nm)	± (nm)
Untreated	246	20
Abrasive paper on a lathe (roughness with preferred orientation)	580	81
Sand blasted	794	74
Etching with HCl (1:3 diluted), 5 min	291	38
Etching with HCl (1:3 diluted), 10–15 min	1300–4300	–

surfaces can be simply predicted by measuring the receding contact angle. Smooth surfaces show a maximum receding contact angle of around 120°. For a further decrease of the ice adhesion, θ_{rec} has to be increased. As stated by Meuler, this is only possible if micro- or nano-structured surfaces are used. Those structured surfaces may show enhanced hydrophobic properties. Since in our paper a superhydrophobic coating did not show an improved icephobic behaviour, we wanted to proof the applicability of Meuler's results to the coatings tested in our study. Therefore six coatings were analyzed in regard of their receding contact angles. Fig. 6 shows the ice adhesion strength of these materials versus the practical work of adhesion scaling parameter $(1 + \cos\theta_{rec})$ in analogy to Meuler's plot. A linear correlation of the adhesive strength on the scaling parameter is notable in the case of the smooth surfaces, however in our case the linear fit does not pass the origin as stated by Meuler. The superhydrophobic coating "Sol–Gel fluorinated + Aerosil 1d" deviates significantly from this linear correlation. Due to the textured surface, the contact angle hysteresis $(\theta_{adv} - \theta_{rec})$ is more pronounced resulting in a relatively small receding contact angle by showing a high static contact angle at the same time.

In sum, the linear correlation of the ice adhesion on $(1 + \cos\theta_{rec})$ in the case of non-textured surfaces was generally confirmed and so, the ice adhesion of those coatings seems to be predictable by knowing the receding contact angle. However, there is still a lack of understanding ice adhesion strengths in regard of superhydrophobic surfaces.

3.3. Influence of roughness on ice adhesion

The question concerning the correlation of surface characteristics and ice adhesion is still not yet fully answered. Depending on the measuring method and icing condition one obtains different results. A superhydrophobic surface does not ice if a supercooled droplet falls on it from a relatively large distance because the droplet will drip off instantly if the surface is tilted [32]. If, however, such a superhydrophobically coated plate is iced by immersing in a vessel filled with water, as in our study, the force required to pull the plate out of the ice is a multiple larger than the one required for an uncoated plate. This depends very much on the structuring of the surface, that is, on the roughness of the coating. In order to obtain a systematic correlation between surface roughness and ice adhesion, the influence of surface roughness has been examined in various ways. In this study aluminium pins were roughened by different methods and their ice adhesion was determined. These pins were further modified with a fluorine-containing coating in order to study the influence of minimized surface energies.

Characterization of surface topography is important in many areas, because roughness influences friction and sliding of surfaces considerably. As with other parameters, the measurement of surface roughness depends very much on the method employed and on the size of the sample area because it is a statistical measure. If one considers the structure of a surface to follow a sinusoidal behaviour, then the amplitude can be taken as roughness and the wavelength as structural feature. In our investigations we focused on mean roughness, which describes the distance of a point to an imaginary middle line. This middle line intersects the profile at the location investigated. Average roughness therefore corresponds to the arithmetic mean of the deviation to the middle line. A popular method to determine roughness parameters is the profile method, where a diamond tip slides over a surface and depicts roughness. A disadvantage of this method is that the needle can deform the surface and therefore alter the roughness. In our study the contactless method of confocal microcopy was used. One obtains a surface related roughness parameter, S_a.

Roughness on the aluminium pins was generated chemically by etching in hydrochloric acid or mechanically by sand blasting or using abrasive paper. Table 1 shows the roughness of samples according to the chosen surface treatments.

It is seen that the untreated pins have quite low roughness. By sand blasting the surface is roughened considerably and this roughness can be reproducibly adjusted. Pins that are treated with abrasive paper on a lathe show a roughness between those that are sand blasted and untreated. With chemical etching, roughness depends on treatment time. Two times were chosen; 5 min or 10–15 min, where most of the time the pins were withdrawn from the acid after 13 min, because thereafter the reaction became uncontrollable. Roughness increases only slightly after 5 min etching time, however, after more than 10 min, one obtains a roughness in the lower micrometre range. Because many pins were etched, those with comparative roughness could be taken together for further experiments. Finally, the condition of each individual pin and the temperature of the acid solution play an important role in the resulting roughness.

The objective is to obtain a relationship between roughness and ice adhesion. First, ice adhesion of the uncoated pins having different roughness was determined. Table 2 shows the corresponding results.

The mechanically treated pins display a clear trend: the rougher the surface, the higher the shear stress at which the ice–aluminium bond is broken (Fig. 7). A higher roughness leads to a larger contact area and the ice can actually anchor itself to the surface. Fig. 7 shows also the maximal shear force that can be achieved with an ice adhesion test totally filled with water ($\tau = 2900$ kPa). This value corresponds to the maximal traction of the tensile test machine of 10 kN. In order to determine higher shear stresses, measurements with half-filled moulds were performed to reduce the contact area between ice and pin and therefore the force required to extract the pin.

Pins which have been treated with acid for 5 min do not display a great increase in roughness. However, their increase in shear stress is considerable. This means that the chemically altered surface

Table 2
Shear stress τ and roughness S_a of different samples without coating.

	Sample	Roughness (nm)	τ (kPa)	$\pm$ (kPa)	ARF
Mechanically treated	Untreated	246	1594	72	1
	Abrasive paper on a lathe (roughness with preferred orientation)	580	2562	430	0.62
	Sand blasted*	794	3901	262	0.41
Chemically treated	Etching with HCl (1:3 diluted), 5 min	291	2681	194	0.6
	Etching with HCl (1:3 diluted), 10–15 min	>1300	>2900	–	≪0.54

* Ice adhesion test totally filled with water exceeded the maximal traction of the tensile test machine. In order to determine shear stresses, measurements with half-filled moulds were performed.
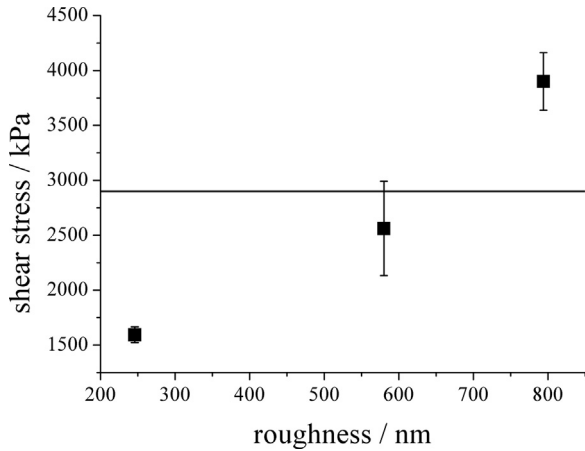

Fig. 7. Dependence of shear stress on roughness of surface treated aluminium pins (only mechanically treated samples); the horizontal line denotes the maximum value of shear stress that can be measured by a completly filled mould.

Fig. 9. Dependence of roughness before and after application of the coating ("sol–gel fluorinated 1"). Thickness of coating is below 1 μm.

displays a strong ice adhesion. Pins that have been etched longer and therefore possess a roughness in the lower micrometre range could not be drawn out of the ice. The enormous roughness and the corresponding increase in surface area leads to a very strong bond to the ice; hence these samples could not be analyzed in this study.

After the determination of ice adhesion to the differently roughened aluminium pins, they were coated with the thin, fluorine containing sol–gel coating "sol–gel fluorinated 1a". This coating displays a certain icephobic character (ARF ≈ 15) on smooth pins, which is attributed to the perfluorinated polyether (Fluorolink®S10) which significantly lowers adhesion. Coating thickness is below 1 μm and therefore not all of the surface
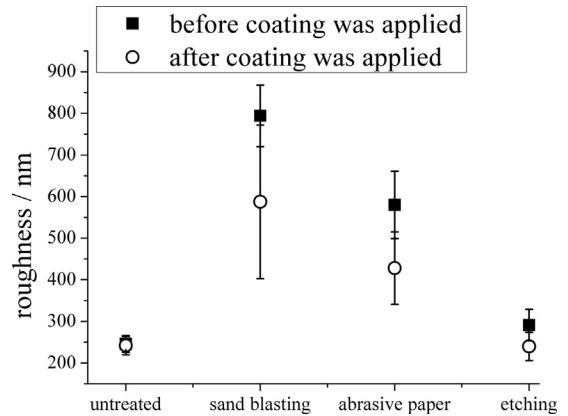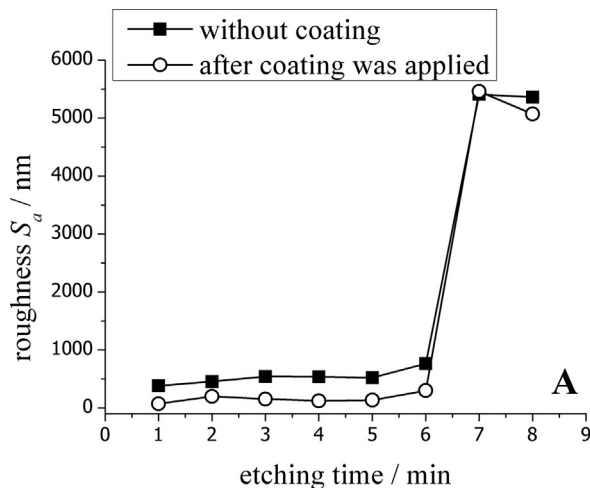
structure is covered. By using this coating, the roughness of the surface is preserved in large parts, although the surface energy is strongly lowered. Additionally, surfaces coated with the fluorine containing sol–gel system become hydrophobic, hence, a rough and low-energy surface is generated. This modification was examined on aluminium platelets. Roughness was determined before and after coating. In Fig. 8 the roughness after coating and the corresponding static contact angles are displayed. It is obvious that the roughness of the surface is slightly reduced by the coating. In case of large roughness there is little change by the coating. The static water contact angles on this coating for smooth surfaces are in the range of 120°. Contact angles higher than 150° and therefore superhydrophobic coatings are obtained if the surface roughness increases to approx. 5 μm. This change of topography in
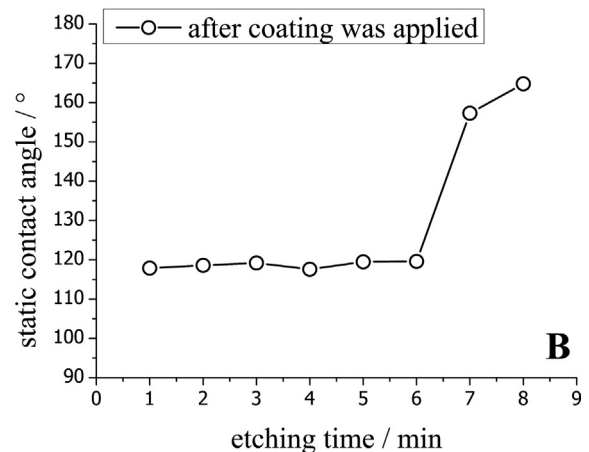

Fig. 8. (a) Dependence of roughness of aluminium platelets on etching time before and after application of coating "sol–gel fluorinated 1"; pickling solution: HCl, 1:4 diluted; (b) course of the corresponding water contact angles.
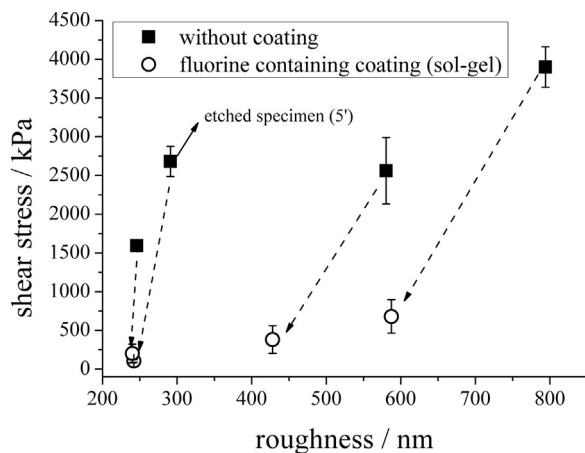
Fig. 10. Dependence of shear stress on roughness before and after application of fluorine containing coating "sol–gel fluorinated 1".

combination with a low energy coating reveals superhydrophobic properties of the surface.

Fig. 9 shows the reduction in roughness caused by coating of the pins. Roughness is only slightly influenced but surface energy is substantially reduced. Therefore, ice adhesion should be lower compared to the uncoated, rough pins. In Fig. 10 ice adhesion is displayed as a function of roughness for coated and uncoated pins. At a first glance it can be seen that the values of the uncoated pins lie above those of the coated pins. With increasing roughness the shear stress necessary to overcome the adhesion of ice to coating increases, and because the coated pins show some roughness, the rougher ones display higher ice adhesion than the smoother ones. A special case is presented by the etched (5 min) pin. Although roughness is relatively small, this sample shows a shear stress of about 2500 kPa.

The coating has clearly a significant influence on ice adhesion. Next to reducing surface energy, roughness is a bit reduced, as seen in Fig. 10, and both factors reduce shear stress.

The coated pins that have been etched for 10–15 min could not be measured. At a roughness above 1 μm a reduction of roughness by about 200 nm carries no weight. Because roughness is preserved on a micrometre scale, the reduction in surface energy barely influences ice adhesion, and the ice can anchor itself well on the surface. For the coated but rough pins 10 kN (maximum load of tensile testing machine) was not sufficient to pull them out of the ice. It is interesting to note that those pins display superhydrophobicity, but although being superhydrophobic, they are not icephobic.

Our results are in good agreement with the study of Zuo et al. They studied aluminium specimens which have been roughened by sand blasting [22]. These specimens were coated with silicon- and fluorine containing coatings, in order to lower surface energy. Ice adhesion was measured with a custom made test whereby a water droplet was frozen onto the surface and ice adhesion was measured using a tip that moves horizontally to detach the ice. The roughness of the untreated aluminium was comparable to that determined in the present study (∼291 nm). However, sand blasting in that study showed a stronger effect and a roughness of about 2.5 μm was obtained. The respective shear stresses showed that an increase in roughness led to higher ice adhesion, in accordance with the results of our study. The applied coatings used by Zuo et al. possessed layer thicknesses of 20–200 nm and therefore the respective roughness is depicted. Their main result was the decrease of shear stresses of coated surfaces due to reduced surface energy. As also shown in our study, lowering the surface energy has a strong influence on shear stress.

4. Conclusion

In this study, various coatings were investigated to analyze their icephobic properties, e.g., hydrophilic and hydrophobic coatings, sol–gel based coatings containing fluorinated compounds and viscoelastic rubbers. Ice adhesion measurements were performed on a custom made $0°$ cone test that showed good reproducibility. It was shown that sol–gel coatings containing fluorinated polyether compounds were able to decrease the adhesion to ice corresponding to an ARF value of about 20. Teflon as a potentially icephobic material possesses an ARF only of seven, standard coatings for wind turbines revealed an ice adhesion character comparable to bare aluminium with very strong adhesion to ice. Quite low adhesion results were obtained in the case of viscoelastic elastomers. A correlation between the static contact angle and the shear stress was not found, but data taken from this study and from AMIL institute showed an excellent agreement. However, a linear correlation of the ice adhesion on $(1 + \cos\theta_{rec})$ of coatings with smooth surfaces was generally confirmed as proposed by Meuler et al. [6]. This relation does not hold for superhydrophobic surfaces and there is a need of further investigations to gain a better understanding of ice adhesion of structured surfaces.

Significantly, a coating of a viscoelastic elastomer (polydimethylsiloxane) showed an outstanding ARF value of about 100, whereas this coating is a permanent one and therefore not time limited like viscoelastic greases or other sacrificial coatings showing equally high ARF values.

In addition to the chemical composition of the surface, the topography of the coatings, namely roughness, has an influence on the adhesive strength to ice. In order to obtain a systematic correlation between surface roughness and ice adhesion the influence of surface roughness has been examined. Different degrees of roughness were created by mechanical and chemical treatment of the aluminium pins. It was shown that the adhesive strength was enhanced by increasing surface roughness. Covering these pins with a fluorinated coating led to a decrease of the surface energy but preserved surface topography. These rough but low energy surfaces showed lower shear stresses, however, rough surfaces still adhered stronger to ice than smoother ones. Those coated pins that showed superhydrophobicity displayed very high adhesive strengths; hence they cannot be considered as icephobic surfaces.

References

[1] O. Parent, A. Ilinca, Anti-icing and de-icing techniques for wind turbines: critical review, Cold Regions Science and Technology 65 (1) (2011) 88–96.

[2] M. Hirayama, K. Siegmann, Antifreeze-Beschichtungen für Rotorblätter, Erneuerbare Energien 11 (2007) 38–41.

[3] R.B. Haehnel, N.D. Mulherin, The Bond Strength of an Ice–Solid Interface Loaded in Shear, in Ice in Surface Waters, Shen, Rotterdam, 1998, pp. 597–604.

[4] N.D. Mulherin, R.B. Haehnel, K.F. Jones, Toward developing a standard shear test for ice adhesion, in: Eight International Workshop on Atmospheric Icing of Structures (IWAIS), Reykjavik, 1998.

[5] S.Q. Yang, et al., Research on the icephobic properties of fluoropolymer-based materials, Applied Surface Science 257 (11) (2011) 4956–4962.

[6] A.J. Meuler, et al., Relationships between water wettability and ice adhesion, ACS Applied Materials and Interfaces 2 (11) (2010) 3100–3110.

[7] L.L. Cao, et al., Anti-icing superhydrophobic coatings, Langmuir 25 (21) (2009) 12444–12448.

[8] P. Tourkine, M. Le Merrer, D. Quere, Delayed freezing on water repellent materials, Langmuir 25 (13) (2009) 7214–7216.

[9] A. Dotan, et al., The relationship between water wetting and ice adhesion, Journal of Adhesion Science and Technology 23 (15) (2009) 1907–1915.

[10] H. Saito, K. Takai, G. Yamauchi, A study on ice adhesiveness to water-repellent coating, Materials Science Research International 3 (3) (1997) 185–189.

[11] S.A. Kulinich, M. Farzaneh, Ice adhesion on super-hydrophobic surfaces, Applied Surface Science 255 (18) (2009) 8153–8157.

[12] S.A. Kulinich, M. Farzaneh, How wetting hysteresis influences ice adhesion strength on superhydrophobic surfaces, Langmuir 25 (16) (2009) 8854–8856.

[13] S.A. Kulinich, et al., Superhydrophobic surfaces: are they really ice-repellent? Langmuir 27 (1) (2011) 25–29.

[14] S. Farhadi, M. Farzaneh, S.A. Kulinich, Anti-icing performance of superhydrophobic surfaces, Applied Surface Science 257 (14) (2011) 6264–6269.
[15] K.K. Varanasi, et al., Frost formation and ice adhesion on superhydrophobic surfaces, Applied Physics Letters 97 (23) (2010).
[16] S. Jung, et al., Are superhydrophobic surfaces best for icephobicity? Langmuir 27 (6) (2011) 3059–3066.
[17] M.F. Hassan, H.P. Lee, S.P. Lim, The variation of ice adhesion strength with substrate surface roughness, Measurement Science and Technology 21 (7) (2010).
[18] W.D. Bascom, R.L. Cottingt, C.R. Singlete, Ice adhesion to hydrophilic and hydrophobic surfaces, Journal of Adhesion 1 (October) (1969) 246.
[19] M.J. Saif, J. Anwar, M.A. Munawar, A novel application of quaternary ammonium compounds as antibacterial hybrid coating on glass surfaces, Langmuir 25 (1) (2009) 377–379.
[20] M. Hirayama, et al., Activated poly(hydromethylsiloxane)s as novel adhesion promoters for metallic surfaces, Journal of Adhesion 72 (1) (2000) 51–63.
[21] C. Laforte, J.-L.C.J.-C. Laforte, How a solid coating can reduce the adhesion of ice on a structure, in: IWAIS 2002, Brno, Czech Republic, 2002.
[22] M. Zou, et al., Effects of surface roughness and energy on ice adhesion strength, Applied Surface Science 257 (8) (2011) 3786–3792.
[23] C. Laforte, A. Beisswenger, Icephobic material centrifuge adhesion test, in: Xi International Workshop on Atmospheric Icing of Structures (IWAIS), Montreal, 2005.
[24] C. Watson, Erosion resistant anti-icing coatings, European Patent Office; to U.T. Corporation, Editor, 2007.
[25] R. Karmouch, et al., Icephobic PTFE coatings for wind turbines operating in cold climate conditions, in: 2009 IEEE Electrical Power & Energy Conference (EPEC 2009), 2009, p. 6.
[26] C. Laforte, A. Beisswenger, Centrifuge Adhesion Test, in: SAE G-12 Future Deicing Technology Subcommittee, Frankfurt, 2004.
[27] P. Fabbri, et al., Surface properties of fluorinated hybrid coatings, Journal of Applied Polymer Science 102 (2) (2006) 1483–1488.
[28] G. Schottner, K. Rose, S. Amberg-Schwab, Hochwertige Kunststoffoberflächen, Kunststoffe 10 (2004) 306–311.
[29] J. Schwarz, S. Svoboda, B. Oertel, Results from sol–gel coatings on austenitic CrNi steel, Materialwissenschaft und Werkstofftechnik 34 (7) (2003) 641–644.
[30] F. Auer, J. Harenburg, C. Roth, Funktionelle Schichten auf Metallen: Massgeschneiderte Eigenschaften durch Sol-Gel-Technologie, Materialwissenschaft und Werkstofftechnik 32 (10) (2001) 767–773.
[31] A. Beisswenger, G. Fortin, C. Laforte, Advances in Ice Adherence and Accumulation Reduction Testing at the Anti-icing Materials International Laboratory (AMIL), in: Future Deicing Technologies, Berlin, 2010.
[32] J. Aizenberg, et al., Design of ice-free nanostructured surfaces based on repulsion of impacting water droplets, ACS Nano 4 (12) (2010) 7699–7707.